Laminar to Turbulent Transition due to unsteady Inflow Conditions: Wind Tunnel Experiments at increased Turbulence Levels

J. Romblad[1], D. Ohno[1], T. Nemitz[2], W. Würz[1], E. Krämer[1]
[1]Institut für Aerodynamik und Gasdynamik der Universität Stuttgart
70550 Stuttgart, romblad@iag.uni-stuttgart.de
[2]Fachgebiet Strömungslehre und Aerodynamik, TU Darmstadt, 64347 Griesheim

Abstract

Within the Luftfahrtforschungsprogramm (LuFo), measurements on a laminar flow airfoil in flight as well as in a wind tunnel are combined with direct numerical simulations (DNS) to provide the base for future improvements of transition prediction under unsteady inflow conditions.

Two regions of turbulent length scales of the inflow are of particular interest for investigating the effect on boundary layer transition on straight wings: large length scales leading to unsteady pressure distributions of the airfoil and small length scales corresponding to the streamwise wave lengths of Tollmien-Schlichting (TS) waves in the boundary layer. The current paper focuses on wind tunnel measurements of the effect of small scale turbulence.

In the Laminar Wind Tunnel of the IAG, small scale turbulence is investigated using an active grid in the settling chamber, enabling measurements at turbulence levels (Tu) ranging from 0.01% (15-5000 Hz) without grid up to 0.11%. The turbulence spectra compare very well with flight measurements in the frequency range relevant for TS-instability. Hot-wire anemometry is used for detailed boundary layer measurement while modified piezoresistive pressure transducers are utilized to measure surface pressures fluctuations up to 8 kHz.

In the range 0.01% ≤ Tu ≤ 0.11% the transition location on the pressure side of the MW-166-39-44-43 airfoil shifts upstream with increasing Tu, the frequency of the most amplified TS waves increases and the transition process change gradually from a quasi-uniform nature to a structure with isolated wave packets. Simultaneously the frequency wavenumber spectrum indicates an increased amount of energy at higher spanwise wave numbers.

The Tu dependent n-factor of the MW-166-39-44-43 airfoil was found to match very well with the modified e^9 method of Mack, while the corresponding n-factor of a XIS40mod airfoil showed a much lower sensitivity, and a close to linear dependency on Tu. A variation in contribution of the receptivity coefficient in the modified e^9 method did not capture the difference in Tu-dependency observed for the two airfoils.

1. Introduction

The reduction of aerodynamic friction drag through extended laminar boundary layer flow enables significant increases in the efficiency of aircraft and wind turbines. Natural laminar flow airfoils are designed to exploit this path. The most commonly used design methodologies (Croach 2015) rely on the prediction of boundary layer transition based on the e^n method, which typically assumes steady boundary conditions. However, airfoils of aircraft and wind turbines are exposed to atmospheric turbulence which results in unsteady inflow conditions.

The spectrum and intensity of atmospheric turbulence has been investigated from various perspectives. For example Shei et al. 1971 measured a very large range of length scales utilizing an aircraft and a meteorology mast, Li et al. 2014 published measurements in low wind conditions as well as strong winds (typhoon), Chougule and Mann 2015 investigated the difference between the turbulence over open terrain and forest and Bodini et al. 2018 used LIDAR to map the turbulence from the ground up to several hundred meters. The results fit well with a spectrum based on the Kolmogorov hypotheses (Kolmogorov 1941) with its three distinct regions: the energy containing range, the inertial subrange and the dissipation subrange (Pope 2000).

Flight measurements of the inflow conditions were performed by Otten et al. 1982 at an altitude ranging from 3.7 km to 12 km. They found very low turbulence levels in the order of 0.02%. Zanin 1984 was probably the first to measure the atmospheric turbulence level with a glider at altitudes below 1200 m. The reported turbulence intensities varied around 0.2% (1-5000 Hz), much higher than Otten et al.

Nitsche et al. 2001, Peltzer 2004 and Seitz and Horstmann 2006 have investigated the transition from laminar to turbulent boundary layer in flight conditions, mainly focusing on low turbulence conditions, i.e. $Tu = u'/U_{inf}$ ≤ 0.05%.

Reeh 2014 performed flight measurements on a natural laminar flow airfoil at different levels of atmospheric turbulence. He proposed to separate the effect of the freestream turbulence into large scale and small scale turbulence. The large scale causes unsteady variations in the inflow angle, which in turn results in unsteady variations of the pressure distribution to which the boundary layer responds. The small scale turbulence enters the boundary layer through receptivity (Morkovin 1977) and provides initial amplitudes of disturbances within the boundary layer.

Field measurements of the transition on wind turbines are less frequent in the literature. Madsen et al. 2010 used surface mounted microphones on an 80 m diameter rotor in the DAN-AERO projects and Schaffarczyk et al. 2014 performed measurements on a 33 m diameter rotor using hot films. Although less conclusive than the mentioned flight investigations, the two measurements on wind turbines show significant portions of laminar boundary layer as well as the atmospheric turbulence influencing the boundary layer transition.

Based on a huge set of wind tunnel tests Kendall 1990 found that below Tu ≤ 0.2-0.5% transition takes place through amplification of Tollmien-Schlichting (TS) waves with wave packets gradually occurring at

©2018

doi:10.25967/480138

increased turbulence. At higher turbulence levels the formation of streaks and low frequency disturbances (Klebanoff modes) tend to dominate the transition process and bypass transition occurs, see the review by Durbin 2017. The upper level of turbulence for which the TS-type transition is dominating is not clear from the literature. Arnal and Juillen 1978 (see also Kendall 1985 and 1998, Matsubara and Alfredsson 2001 and Fransson 2017) reported TS-waves at Tu = 0.1%, but at Tu = 0.3% the waves were barely distinguishable. At Tu = 1.0% the transition scenario was dominated by unsteady streamwise streaks. Suder and O'Brian 1988 found TS-type transition at Tu = 0.3%, while at 0.65% bypass transition was prevailing. Beside the importance of the spectral energy distribution covered by the integral Tu level, this points at TS-waves being the relevant transition mechanism for small scale turbulence in the range of interest for low to moderate atmospheric turbulence (Tu up to around 0.1%).

The ongoing project "Laminar-turbulente Transition unter instationären Anströmbedingungen", supported by the Luftfahrtforschungsprogramm (LuFo), is focusing on the effects of atmospheric turbulence on boundary layer transition with the target of improved understanding of the underlying mechanisms. Measurements on a natural laminar flow airfoil are performed both in flight and in the wind tunnel. Together with results from direct numerical simulation (DNS) the measurements will provide a base for future improvements of transition prediction under unsteady inflow conditions.

This paper describes wind tunnel investigations of the stationary base flow and the impact of increased levels of small scale turbulence.

2. Measurement setup and data acquisition

2.1. Wind tunnel and airfoil models

The measurements were performed in the Laminar Wind Tunnel (LWK) of the Institute for Aerodynamics and Gas Dynamics (IAG) in Stuttgart. The wind tunnel has an open return and a closed test section with a cross section of 0.73 x 2.73 m^2 and a length of 3.15 m. The base turbulence level is very low due to the high contraction ratio (effectively 20:1) and the use of several screens and filters in the inlet part of the tunnel. At 38 m/s the base turbulence level is 0.01% in the range 15-5000 Hz. The background noise level is kept low through sound absorbing lining in the first part of the diffuser (Plogmann and Würz 2013).

The airfoil used for the main part of the investigations is a MW-166-39-44-43 natural laminar flow airfoil of 1.35 m chord. The 6 mm thick fibreglass and carbon fibre shells were manufactured in the same negative moulds as the wing-glove used for the flight measurements, allowing wind tunnel measurements at flight Reynolds numbers.

The model is equipped with 42 pressure taps with 0.4 mm diameter which are distributed from x/c = 0.01 on the suction side to x/c = 0.73 on the pressure side. The taps upstream of x/c = 0.05 are offset 20° in spanwise direction to minimize disturbance between taps. A spanwise row of 14 pressure taps with 7 mm spacing is located at x/c = 0.311. At each end of the row a flush mounted Kulite XCQ-062-5D is used as reference pressure transducer.

A small influence on the transition was produced by the pressure taps upstream x/c = 0.15 and for most of the measurements these taps were closed by a 40 µm thick and 12 mm wide adhesive tape. For the transition detection measurements with IR thermography those taps were sealed with gelcoat and the surface sanded smooth.

A universal disturbance source is located at x/c = 0.15. The disturbance source was not used in the current measurements and was sealed by a 40 µm thick and 12 mm wide adhesive tape for most of the measurements. For the transition detection measurements with IR thermography the slit was sealed with an elastic polyurethane compound (Teroson PU-92) which was sanded to match the airfoil contour.

Additional measurements were performed on a 0.6 m chord XIS40mod airfoil model which is of similar construction as the MW-166-39-44-43. The XIS40mod is a symmetric, 15% maximum thickness airfoil designed for transition investigations, see Würz 1995 for details.

2.2. Data acquisition and processing

Three main measurement techniques have been used for the present investigations: surface pressures (both steady and unsteady), hot-wire anemometry (in the boundary layer or the freestream) and infrared thermography.

Steady surface pressures were measured at all pressure taps by a PSI ESP64HD pressure scanning module.

Unsteady surface pressures were measured at every second pressure tap using discrete piezoresistive transducers (SensorTechnics HCL0050T) which have been modified to reduce the internal volume and to allow an installation similar to Franzoni and Elliott 1998 and Perennes and Roger 1998, using the 2.0 m long tube to the PSI pressure scanner as damping pipe. This effectively connects the discrete HCL transducer and PSI unit in parallel, allowing measurements with both systems simultaneously. The transducer modifications, the special installation and a frequency dependent calibration enable measurements of unsteady pressures up to 8 kHz.

The signals from the HCL transducers were split in a DC part and an AC part and amplified by low noise amplifiers (Cosytec BRVST2).

Boundary layer hot-wire measurements have been conducted with a DANTEC 55P15 single hot-wire probe with a 5 µm wire controlled by a DISA 55M10 constant temperature anemometer (CTA). The probe was positioned using a computer controlled traversing unit with a traversing accuracy of 5 µm in wall normal direction and 100 µm in spanwise direction.

The hot-wire signal was divided in a DC and an AC part where the AC part was high pass filtered at 50 Hz and amplified depending on the signal level by an AMI 351A-1-50-NI amplifiers.

The signals from both the unsteady surface pressure transducers and the boundary layer hot-wire were acquired using an 80 channel, 16 bit NI USB-6255 AD-converter sampling at 15650 Hz. Low pass filters with 4.8 kHz corner frequency were used for anti-aliasing.

The freestream turbulence was measured using a separate measurement system consisting of a straight

©2018

hot-wire probe with a 2.5 µm diameter wire, a DISA 55M10 CTA anemometer, an AMI 321A-3-50-NI amplifier and a low pass filter with corner frequency of 15 kHz for signal conditioning. The signal was acquired using the 24 bit Sigma-Delta ADC inputs of a RME Hammerfall Mulitface DSP sampling at 44.1 kHz.

A FLIR X6540sc IR camera was used to determine the transition location. The maximum of the temperature gradient in streamwise direction was used to define the transition location.

For the comparison of the experimental results with linear stability theory (LST) a three step procedure was used: i) viscid pressure distributions were calculated by XFOIL V6.96, ii) Based on these distributions the boundary layer parameters were determined using a finite differential scheme (Cebeci and Smith 1974) and iii) the Orr-Sommerfeld equation was addressed with a shooting solver (Conte 1966).

2.3. Turbulence generation

Small scale turbulence is generated by an active, pneumatic grid according to the method described by Kendall 1990 where the grid is placed in the settling chamber of the wind tunnel. The 2 m by 2 m grid consists of 2 mm horizontal tubes with 0.2 mm diameter holes which generate tiny jets blowing upstream as compressed air is applied through the tubes of the grid. The pressure level of the supplied air controls the resulting turbulence level in the test section. At u_{inf} = 38 m/s a turbulence level between 0.03% and 0.11% can be set (Tu = 0.01% without grid).

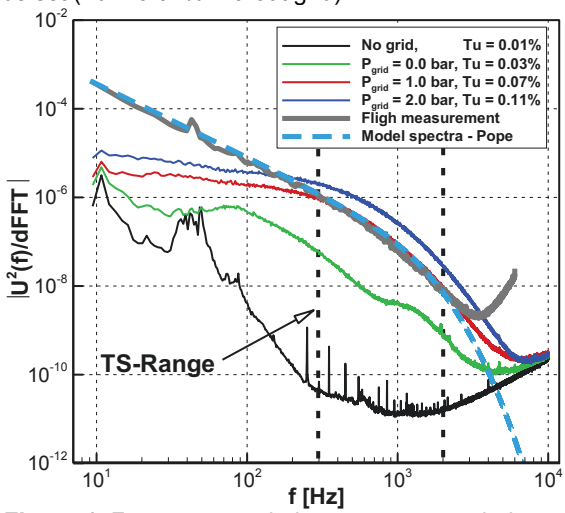

Figure 1. *Freestream turbulence spectrum wind tunnel (with and without active grid), in flight and model spectrum.*

Figure 1 shows the frequency spectrum of the freestream turbulence with and without the grid. Compared to flight measurements and a model spectrum according to Pope 2000 the wind tunnel spectrum captures the dissipative subrange above 400 Hz very well. Toward lower frequencies the flight measurements show a clear inertial subrange with the familiar -5/3 exponent slope. In this range the slope of the spectrum from the wind tunnel is less steep and the two spectra gradually diverge below 400 Hz. In the current experiment Tollmien-Schlichting amplification occurs in a range of frequencies 300 ≤ f ≤ 2000 Hz in which the inflow measurement in the atmosphere and the wind tunnel matches well.

3. Results and discussion

3.1. Base flow - low turbulence level (Tu = 0,01 %)

A reference case of $\propto$= -1.4° and Re = $3.4 \cdot 10^6$ has been selected based on the measured conditions for cruise/dash flight close to the lower corner of the laminar bucket of the airfoil. All measurements are made on the pressure side of the airfoil which is the most sensitive side for the selected reference condition. To compensate for the influence of the wind tunnel walls, the angle of attack of the wind tunnel model has been adjusted to match the measured pressure gradient with a RANS calculation of the simulated flight condition in the range 0.05 < x/c < 0.4. As can be seen

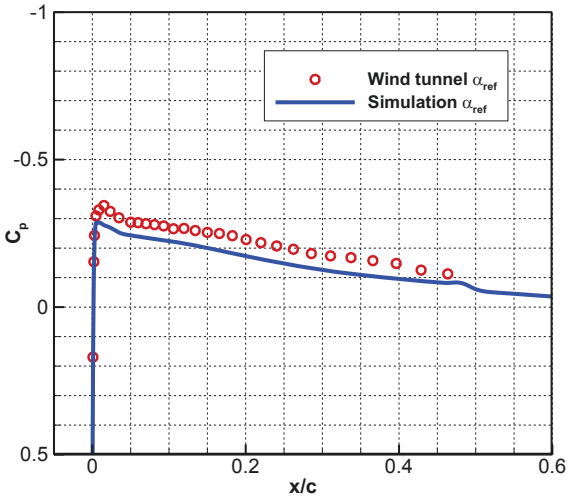

Figure 2. *Pressure distribution from measurement and RANS simulation.*

in figure 2 an offset remains in the pressure distribution although this is not regarded as important for the boundary layer development. Hereafter $\boldsymbol{\alpha_{ref}}$ will be used for -1.4° angle of attack in free flight and simulations as well as for -0.7° geometric angle of attack in the wind tunnel.

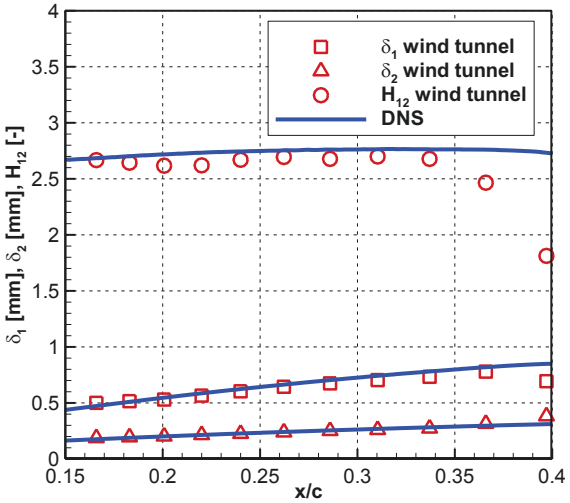

Figure 3. *Mean boundary layer parameters from measurement and DNS.*

Figures 3 shows the measured mean boundary layer parameters compared with DNS. The measured

displacement thickness δ_1 and shape factor H_{12} lies slightly below the simulations while the momentum thickness δ_2 matches very well. The drop in H_{12} at transition occurs earlier in the experiment than in the simulations.

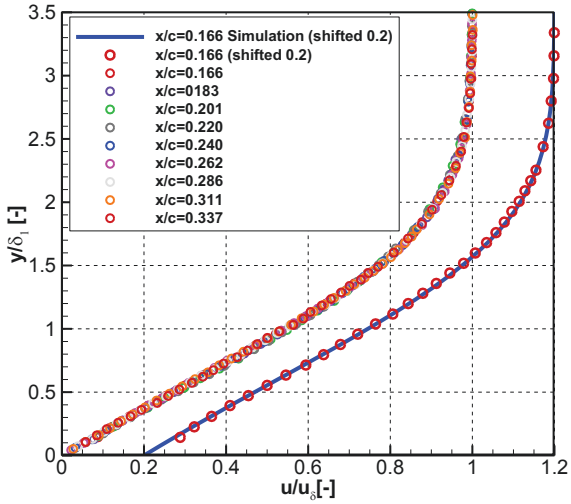

Figure 4. *Measured boundary layer velocity profiles.The profile at x/c= 0.166 is compared with DNS (both shifted by 0.2 to the right for clarity).*

The normalized boundary layer profiles from x/c = 0.166 through x/c = 0.337 in figure 4 show a close similarity which is to be expected from the near constant shape factor H_{12} and the match with DNS results is good.

The hot-wire traversing unit and the adhesive tape over the universal disturbance and pressure taps upstream of x/c = 0.15 had an effect on the transition which explains the shift in transition location between the measurements with hot-wire, unsteady surface pressures (without hot-wire traversing unit) and IR thermography (no hot-wire traversing unit or tapes). Since the measured amplification rates with both the hot-wire traversing unit and tape over the disturbance

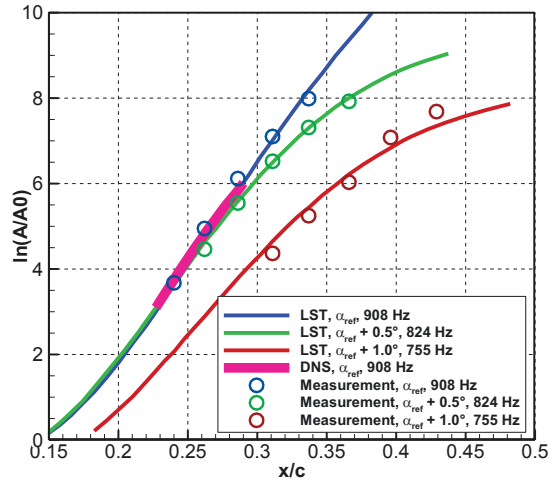

Figure 5. *Comparison of measured amplification rates to LST and DNS.*

source present (figure 5) match well with linear stability theory and the DNS results it is assumed that the influence can be regarded as an increase of the initial disturbance level A_0 due to local receptivity and that the stability characteristics of the boundary layer remains the same as without hot-wire traverse unit and the tapes.

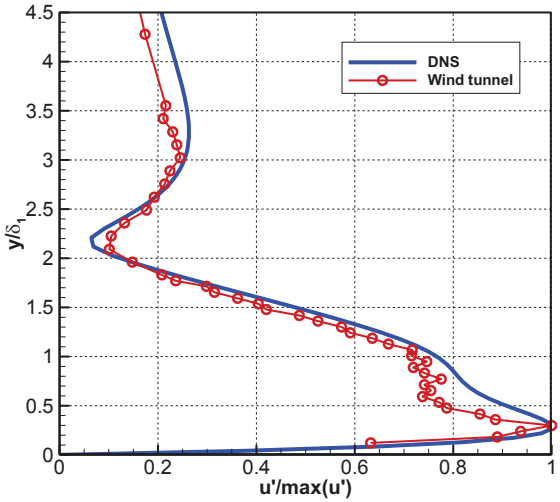

Figure 6. *Eigenfunctions from measurement and DNS. x/c = 0.262, $\propto_{ref}$, f = 908 Hz, 2D waves used in simulation.*

In figure 6 the measured eigenfunction at x/c = 0.262 and f = 908 Hz is compared to DNS results for a 2D wave. Since the experimental eigenfunction is a composition of 2D and 3D waves, differences are visible close to the second wall near maximum.

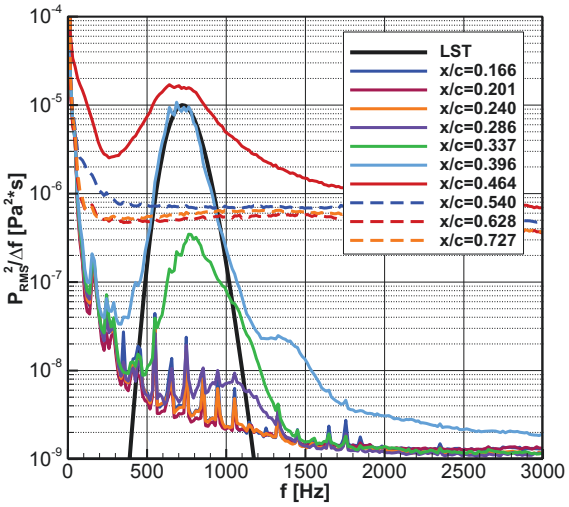

Figure 7. *Spectra of unsteady surface pressures compared with 2D LST for x/c = 0.396.*

The downstream evolution of spectra from the unsteady surface pressures (figure 7) show a first Tollmien-Schlichting "hump" with a centre frequency of about 1000 Hz visible above the electric noise floor at x/c = 0.286. TS frequencies are further amplified downstream with a shift to lower frequencies. At x/c = 0.396 higher harmonics continuous appear and at x/c = 0.464 strong non-linear effects are seen with a fill-up of the spectrum at frequencies both below and above the most amplified frequencies. Downstream x/c = 0.540 the typical spectrum of a turbulent boundary layer emerges.

A direct comparison with linear stability theory is difficult due to the mixture of 2D and 3D waves, but a coarse comparison of spectra at x/c = 0.396 show a very good agreement in frequency range. The LST spectrum is based on a flat A_0 distribution with an initial

©2018

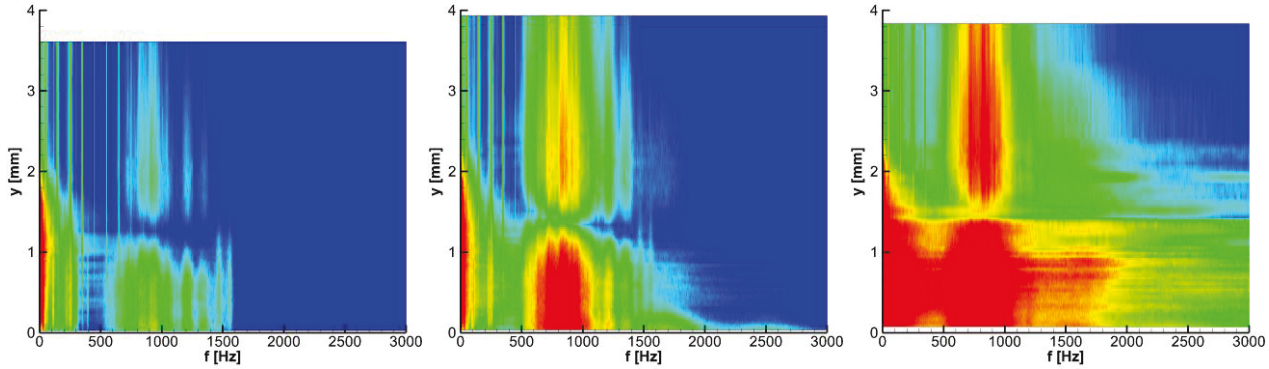

Figure 8. *Measured wall normal spectra at a) x/c = 0.262, b) x/c = 0.311 and c) x/c = 0.337.*

amplitude adjusted to match the peak amplitudes of the LST and the experiment.

The wall normal spectra (figure 8) show a linear stage at positions x/c = 0.262 and 0.311 with amplification of TS-modes and typical TS-wave eigenfunctions. At x/c = 0.337 a non-linear stage can be seen with the above described fill-up of the spectrum at frequencies outside the TS-region. This is as expected in a classic TS-wave transition at low turbulence levels and a moderate adverse pressure gradient.

The spanwise wave number spectra of the unsteady surface pressures at x/c = 0.311 and $\propto_{ref}$ (figure 9a) correspond well with the energy spectra from linear stability theory (figure 9b, spanwise wave number independence of the transfer function to surface pressure assumed) in the region of most amplified frequencies. The measurement shows lower amplitudes for larger wave numbers than the LST and some non linear mode amplification can be seen for small wave numbers around 600 Hz and 1400 Hz. The main characteristics of the wavenumber spectrum matches with the spectrum measured on the same airfoil in flight at x/c = 0.482 and ∝= -0.92° (slightly earlier in the transition process) by Reeh 2014.

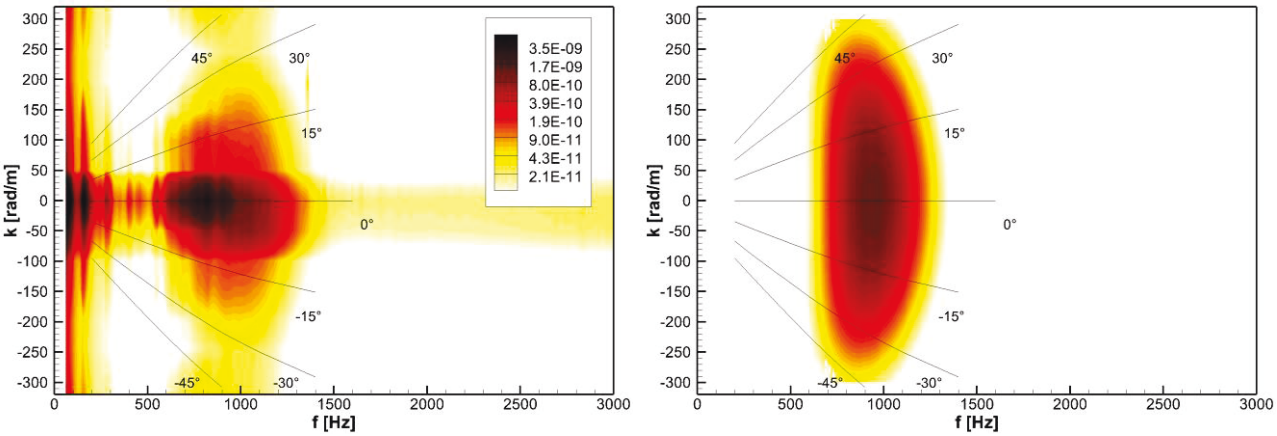

Figure 9. *Frequency wavenumber spectra at x/c = 0.311. a) measured wall pressure fluctuations b) LST energy spectrum.*

3.2. Effects of increased small scale turbulence

As can be seen in figure 10, an increase of the freestream turbulence level reduces the maximum TS-amplitudes and the "TS-hump" broadens. The transition location moves forward and the frequency of the TS-maximum is shifted upwards. The shift in frequency is at least partly attributed to the linear stability

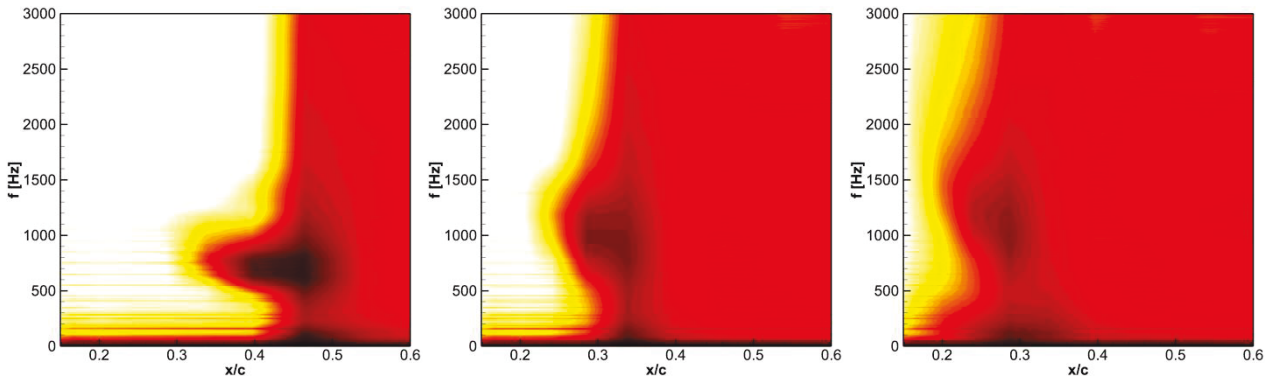

Figure 10. *Measured wall pressure fluctuations at increased turbulence level. a) Tu = 0.01%, b) Tu = 0.05% and c) Tu = 0.11%.*

©2018

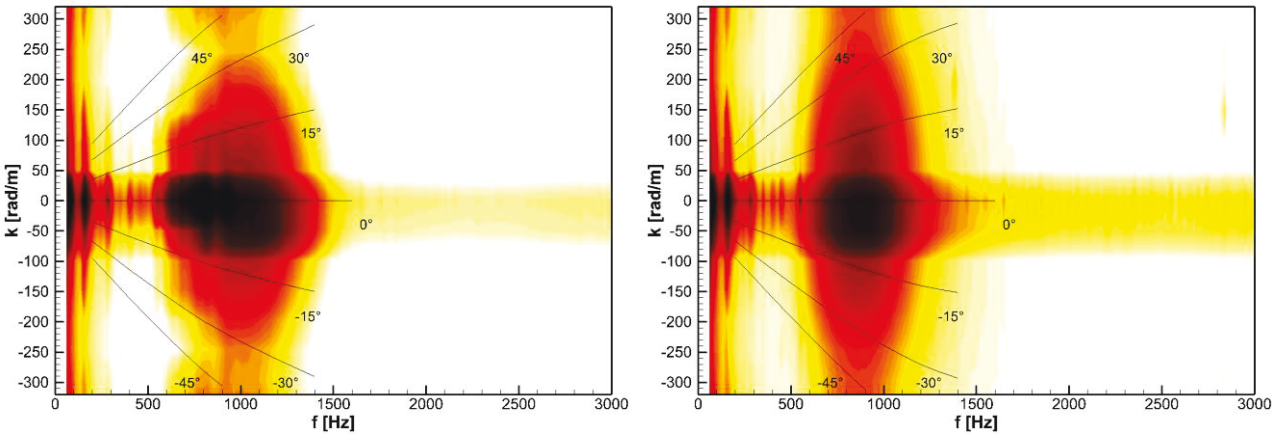

Figure 11. *Frequency wavenumber spectra at x/c = 0.311. a) Tu = 0.01%, $\propto_{ref}$-0.2°, b) Tu = 0.07%, $\propto_{ref}$+1.0°*

characteristics as the amplification of higher frequencies is favoured at upstream positions (compare figure 7).

Comparing spanwise wavenumber spectra for different turbulence levels is somewhat difficult since the transition location moves with turbulence level and a fixed spanwise row of surface pressure taps exists. Therefore figure 11 shows approximately the same stage in the transition process at Tu = 0.01% and 0.07%. The angle of attack has been adjusted to position the transition in relation to the spanwise row of pressure taps ($\boldsymbol{\alpha = \alpha_{ref}}$ - 0.2° and $\boldsymbol{\alpha = \alpha_{ref}}$+1.0° respectively). The procedure is somewhat coarse, but an increase of amplitudes at higher spanwise wavenumbers can be seen in the case with higher freestream turbulence.

measurements by Seitz and Horstmann 2006 at an estimated Tu ≤ 0.05%.

The effect of freestream turbulence on the transition location has been measured in parallel using IR thermography and corresponding n-factors have been determined using linear stability theory. The main advantage of this non-intrusive method is the full spanwise-streamwise information which allows identifying and avoiding regions with high receptivity, e.g. pressure taps. The results are compared to the modified e^9 method of Mack 1997 in figure 13. It should be noted that the method of Mack is based on flat plate measurements and that the data used by Mack showed little change in critical n-factor below Tu = 0.1%, an effect typically attributed to the sound component of the disturbance environment in the wind tunnel controlling

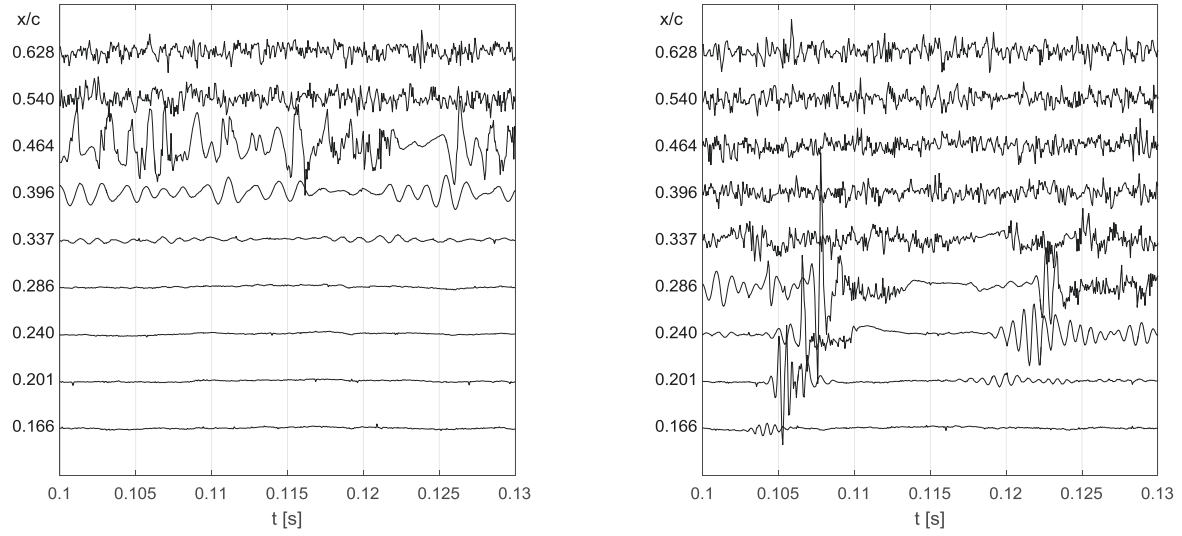

Figure 12. *Time traces of surface pressures at a) Tu = 0.01% and b) Tu = 0.11%.*

The time traces of the unsteady pressure taps in streamwise direction reveal a change in the structure of the transition process from the quasi-uniform nature at Tu = 0.01% (figure 12a) to a structure with formation of isolated wave packages which grow into turbulent spots at Tu = 0.11% (figure 12b). The change is gradual over the 0.01% - 0.11% range of turbulence in the present investigation. The forming of wave packets has been observed by Kendall 1990 when increasing the freestream turbulence from Tu = 0.03% to Tu > 0.1% and wave packets were observed in flight

the transition (Mack 1977) at low Tu. Consequently the valid range for the method is given as Tu > 0.1%.

Although the current transition location measurements on the MW-166-39-44-43 have been performed in the range 0.03% ≤ Tu ≤ 0.11%, there is a very good match with the curve of the modified e^9 method. In the measured range, n_{tr} changes from 11.8 to 8.1 and the gradient steepens toward lower turbulence levels. Measurements in a slightly different configuration (data not included here) indicates that the trend continues also down to Tu = 0.01%.

©2018

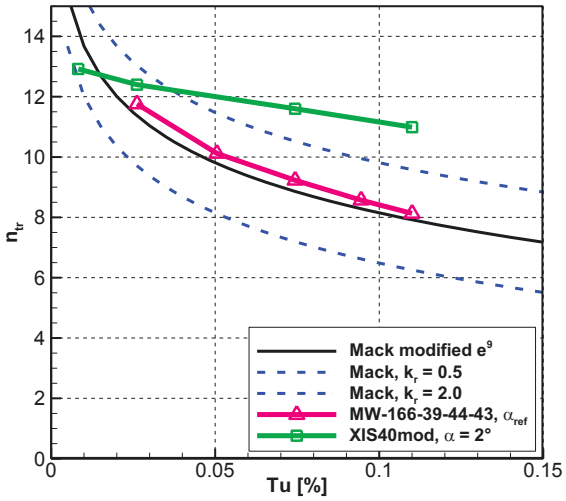

Figure 13. *n-factors at transition for the two airfoils compared with the modified e^9 method of Mack and with the Mack method including the effect of variations in receptivity coefficient.*

The good match between the current measurements at Tu < 0.1% and the modified e^9 method could be linked to the low level of acoustic noise in the LWK wind tunnel (72 dBA at 39 m/s, Plogmann and Würz 2013), leaving the freestream turbulence as the dominating disturbance source at lower turbulence levels than seen in the data used by Mack.

The method of Mack is essentially based on the idea of a constant receptivity factor for transformation of outer disturbances into TS-waves, a linear amplifier (LST) and a amplitude threshold at transition. When using this method on airfoils instead of flat plates, one can assume that the receptivity factor is different.

In order to investigate the influence of the receptivity coefficient on Mack's modified e^9 method, a ratio between receptivity coefficients is defined as

$$k_r = \frac{G_{current}}{G_{Mack}}$$

where G_{Mack} and $G_{Current}$ are the receptivity coefficients in the experiment used my Mack and in the current measurement respectively. Introducing the receptitvity coefficient ratio k_r into the equation of Mack yields

$$n_{tr} = -8.43 - 2.4 \cdot ln(k_r \cdot Tu)$$

Evaluating this expression for different k_r shows that a change in the receptivity coefficient results in a vertical shift of the n-factor curve (figure 13). This means that a change in receptivity coefficient moves the transition similar to a change in Tu.

To get an impression of the applicability of the modified e^9 method to other base flows, IR transition location measurements have been conducted on a XIS40mod airfoil at $\propto$= 2° and Re = 1.5·10^6 (figure 14). The results show a different behaviour of the n-factor compared to the MW-166-39-44-43, see figure 13. In the range 0.01% ≤ Tu ≤ 0.11% n_{tr} changes from 12.9 to 11.0, less than half of the n_{tr} variation seen on the MW-166-39-44-43. In addition n_{tr} varies almost linear with Tu over the measured range, a quite different behaviour compared to the MW-166-39-44-43 for which the gradient increases towards smaller Tu.

The differences in the base flow between the two airfoils causes a significant difference in the response to freestream turbulence level. The difference manifests itself as a change in slope and curve form and is not captured by a change in the receptivity coefficient. The mechanism behind these differences has not yet been clarified.

4. Conclusions

Measurements of the boundary layer transition on the MW-166-39-44-43 natural laminar flow airfoil at unsteady inflow conditions have been performed in the Laminar Wind Tunnel at the IAG, University of Stuttgart.

As small scale turbulence is increased from 0.01% to 0.11% the transition location shifts upstream, the frequency of the amplified TS waves increases and the transition process changes gradually from a quasi-uniform nature to a structure with isolated wave packets. The frequency wavenumber spectrum indicates an increased amount of energy at higher spanwise wave numbers.

In the range 0.03% ≤ Tu ≤ 0.11% the n-factor of the MW-166-39-44-43 airfoil was found to match very well with the modified e^9 method of Mack 1997. In contrast a XIS40mod airfoil showed a much smaller change in n-factor, less than half compared to the MW-166-39-44-43 and with a close to linear dependency of Tu. The difference in response to freestream turbulence between the two airfoils is not captured by a variation of the receptivity coefficient since the contribution of the receptivity shifts the level of the n-factor curve but does not affect the slope of the curve.

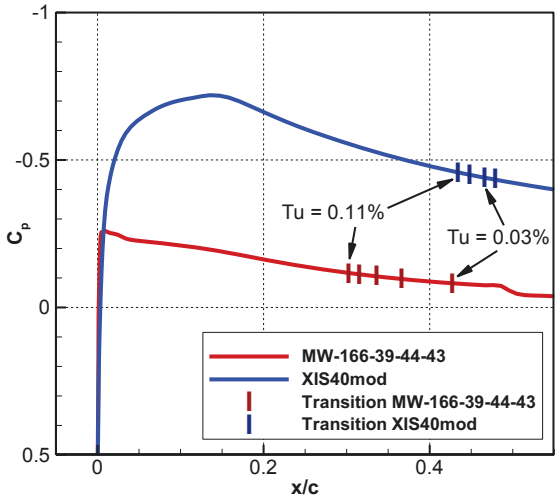

Figure 14. *Pressure distributions calculated with XFOIL and measured transitions locations for different Tu.*

Affiliation

The presented work has been carried out in the project "Laminar-turbulente Transition unter instationären Anströmbedingungen", LTT-USTUTT, Förderkennzeichen 20E1503C supported by the Luftfahrtforschungsprogramm (LuFo) of the Bundesministerium für Wirtschaft und Industrie.

©2018

Gefördert durch:

aufgrund eines Beschlusses
des Deutschen Bundestages

References

Aagaard Madsen, H., Bak, C., Schmidt Paulsen, U., Gaunaa, M., Fuglsang, P., Romblad, J., ... Jensen, L. (2010). The DAN-AERO MW experiments: final report. Risø-R-1726(EN). Danmarks Tekniske Universitet, Risø Nationallaboratoriet for Bæredygtig Energi, available at: orbit.dtu.dk.

Arnal, D., Juillen, J. C. (1978). Contribution Experimentale a l'Etude de la Receptivite d'une Couche Limite Laminaire, a la Turbulence de l'Ecoulement General. ONERA, Rapport Technique, (1/5018).

Bodini, N., Lundquist, J. K., Newsom, R. K. (2018). Estimation of turbulence dissipation rate and its variability from sonic anemometer and wind Doppler lidar during the XPIA field campaign. Atmospheric Measurement Techniques, 11(7), 4291-4308.

Cebeci, T., Smith, A. M. O., (1974). Analysis of Turbulent Boundary Layers, Academic Press, ISBN 0121646505.

Chougule, A., Mann, J., Segalini, A., Dellwik, E. (2015). Spectral tensor parameters for wind turbine load modeling from forested and agricultural landscapes. Wind Energy, 18(3), 469-481.

Conte, S. D. (1966). The numerical solution of linear boundary value problems. Siam Review, 8(3), 309-321.

Crouch, J., 2015. Boundary-layer transition prediction for laminar flow control. In 45th AIAA Fluid Dynamics Conference (p. 2472).

Durbin, P. A. (2017). Perspectives on the Phenomenology and Modeling of Boundary Layer Transition. Flow, Turbulence and Combustion, 99(1), 1-23.

Fransson, J. H. (2017). Free-stream turbulence and its influence on boundary-layer transition. In 10th International Symposium on Turbulence and Shear Flow Phenomena, TSFP 2017, Swissotel ChicagoChicago, United States, 6 July 2017 through 9 July 2017 (Vol. 2). International Symposium on Turbulence and Shear Flow Phenomena, TSFP10.

Franzoni, L. P., Elliott, C. M. (1998). An innovative design of a probe-tube attachment for a 1 2-in. microphone. The Journal of the Acoustical Society of America, 104(5), 2903-2910.

Kendall, J. (1985, July). Experimental study of disturbances produced in a pre-transitional laminar boundary layer by weak freestream turbulence. In 18th Fluid Dynamics and Plasmadynamics and Lasers Conference (p. 1695).

Kendall, J. (1990, June). Boundary layer receptivity to freestream turbulence. In 21st Fluid Dynamics, Plasma Dynamics and Lasers Conference (p. 1504).

Kendall, J. (1998). Experiments on boundary-layer receptivity to freestream turbulence. In 36th AIAA Aerospace Sciences Meeting and Exhibit (p. 530).

Kolmogorov, A. N. (1941, February). The local structure of turbulence in incompressible viscous fluid for very large Reynolds numbers. In Dokl. Akad. Nauk SSSR (Vol. 30, No. 4, pp. 299-303).

Li, S. W., Tse, K. T., Weerasuriya, A. U., Chan, P. W. (2014). Estimation of turbulence intensities under strong wind conditions via turbulent kinetic energy dissipation rates. Journal of Wind Engineering and Industrial Aerodynamics, 131, 1-11.

Loehrke, R. I., Morkovin, M. V., Fejer, A. A. (1975). Transition in nonreversing oscillating boundary layers. Journal of Fluids Engineering, 97(4), 534-549.

Mack, L. M., (1977), Transition and laminar instability. JPL Publication 77-15, NASA-CP-153203.

Matsubara, M., Alfredsson, P. H. (2001). Disturbance growth in boundary layers subjected to free-stream turbulence. Journal of fluid mechanics, 430, 149-168.

McCroskey, W. J. (1981). The phenomenon of dynamic stall (No. NASA-A-8464, TM-81264). NASA AMES.

Morkovin, M. V. (1978). Instability, transition to turbulence and predictability (No. AGARD-AG-236). Advisory group for aerospace research and development neuilly-sur-seine (france).

Nitsche, W., Suttan, J., Becker, S., Erb, P., Kloker, M., Stemmer, C. (2001). Experimental and numerical investigations of controlled transition in low-speed free flight. Aerospace science and technology, 5(4), 245-255.

Obremski, H. J., Fejer, A. A. (1967). Transition in oscillating boundary layer flows. Journal of Fluid Mechanics, 29(1), 93-111.

Otten, L. J., Pavel, A. L., Rose, W. C., & Finley, W. E. (1982). Atmospheric turbulence measurements from a subsonic aircraft. AIAA Journal, 20(5), 610-611.

Peltzer, I. (2004). Flug-und windkanalexperimente zur räumlichen entwicklung von tollmien-schlichting-instabilitäten in einer flügelgrenzschicht (Doctoral dissertation, Technische Universität Berlin). Mensch-und-Buch-Verlag.

Perennes, S., Roger, M. (1998). Aerodynamic noise of a two-dimensional wing with high-lift devices. In 4th AIAA/CEAS aeroacoustics conference (p. 2338).

Plogmann, B., Würz, W. (2013). Aeroacoustic measurements on a NACA 0012 applying the Coherent Particle Velocity method. Experiments in fluids, 54(7), 1556.

Pope, S. (2000). Turbulent Flows. ISBN: 0-521-59125-2. Cambridge University Press.

©2018

Reeh, A. D. (2014). Natural laminar flow airfoil behavior in cruise flight through atmospheric turbulence (Doctoral dissertation, Technische Universität Darmstadt).

Schaffarczyk, A. P., Schwab, D., Ingwersen, S., Breuer, M. (2014). Pressure and hot-film measurements on a wind turbine blade operating in the atmosphere. In Journal of Physics: Conference Series (Vol. 555, No. 1, p. 012092). IOP Publishing.

Seitz, A., Horstmann, K. H. (2006). In-flight investigations of tollmien-schlichting waves. In IUTAM Symposium on One Hundred Years of Boundary Layer Research (pp. 115-124). Springer, Dordrecht.

Sheih, C. M., Tennekes, H., Lumley, J. L. (1971). Airborne Hot-Wire Measurements of the Small-Scale Structure of Atmospheric Turbulence. The Physics of Fluids, 14(2), 201-215.

Studer, G., Arnal, D., Houdeville, R., Seraudie, A. (2006). Laminar–turbulent transition in oscillating boundary layer: experimental and numerical analysis using continuous wavelet transform. Experiments in fluids, 41(5), 685-698.

Suder, K. L., Obrien, J. E., Reshotko, E. (1988). Experimental Study of Bypass Transition in a Boundary Layer. MS Thesis.

Würz, W. (1995), Hitzdrahtmessungen zum laminar-turbulenten Strömungsumschlag in anliegenden Grenzschichten und Ablöseblasen sowie Vergleich mit der Linearen Stabilitätstheorie und empirischen Umschlagskriterien (Doctoral dissertation, Universität Stuttgart)

Zanin, B. Y. (1985). Transition at natural conditions and comparison with the results of wind tunnel studies. In Laminar-Turbulent Transition (pp. 541-546). Springer, Berlin, Heidelberg.

©2018